

# The association of dosimetric quantities from computed tomography with operational factors: basis for optimization strategies

Rafael Alejandro Miller Clemente<sup>1</sup>, Marlén Pérez Díaz<sup>2</sup>

<sup>1</sup> Group of Radiation Medical Physics. Biophysics Dept. Centro de Biofísica Médica, Universidad de Oriente, Santiago de Cuba, Cuba

<sup>2</sup> Electric Engineering Faculty, Universidad Central 'Marta Abreu', Las Villas, Santa Clara, Cuba.  
rafael.miller@uo.edu.cu

## Abstract

Clinical Computed Tomography (CT) imaging is supported by a patient – technology – observers system. Such system involves dosimetric quantities associated with image quality descriptors, where operational factors are predictors. Knowledge of quantitative association between CT dosimetric and image quality quantities with systemic factors, provides the basis to devise scanner-specific optimization strategies. Kerma indexes were measured with a pencil ionization chamber free in air  $C_{a,100}$  and in phantom  $C_{pmma,x}$  (x changes into c and p for center and periphery respectively). Polymethyl Methacrylate (PMMA) standard phantoms were used (diameters of 16 and 32 cm). Several operational factors of a Siemens Sensation 64 Cardiac were considered: estimated spectrums, tube potential  $F_8$  (80 - 140 kV), tube current x time product  $F_1$  (40 - 350 mAs) and total collimation at isocenter  $F_3$  (2,7 - 19,2 mm). The water equivalent radius  $R_w$ , an important factor for patient Size Specific Dose Estimators (SSDE), was estimated by taking into account the spectrums in each phantom. Average pixel noise was measured from Regions of Interest (ROIs) in water phantoms with radius of 2,5; 3; 6; 8 and 11,5 cm. A linear association was found between  $C_{pmma,p}$  and  $C_{pmma,c}$ . A dose reduction of  $C_{pmma,c} = 2$  mGy per tube rotation can be obtained from data analysis (head mode), with  $F_1 = 50$  mAs,  $F_3 = 19,2$  mm, resulting in average pixel noise of 20 Hounsfield Units (HU). Knowledge of noise association with  $C_{pmma,c}$  provides a straightforward tool for quantitative optimization, considering a systemic approach, which includes patient - technology - observer factors.

**Key words:** optimization; dosimetry; X-ray spectra; computerized tomography; image processing.

## Asociación de magnitudes dosimétricas de tomografía computarizada con factores operacionales: bases para estrategias de optimización

### Resumen

La tomografía computarizada (TC) clínica se basa en un sistema paciente – tecnología – observador. Dicho sistema incluye magnitudes dosimétricas asociadas a descriptores de calidad, donde los factores operacionales son predictores. Conocer la asociación cuantitativa entre magnitudes dosimétricas y de calidad de imagen con factores sistémicos, provee la base para concebir estrategias de optimización específicas por tomógrafo. Se midieron índices de kerma en aire  $C_{a,100}$  y en maniquí  $C_{pmma,x}$  (x cambia a c y p para centro y periferia respectivamente) con una cámara de ionización tipo lápiz. Se utilizaron maniqués de Polimetil Metacrilato (PMMA) con diámetros de 16 y 32 cm. Se consideraron factores operacionales de un equipo Siemens Sensation 64 Cardiac: espectros estimados, tensión del tubo  $F_8$  (80 - 140 kV), producto corriente x tiempo de exposición  $F_1$  (40 - 350 mAs) y colimación total en isocentro  $F_3$  (2,7 - 19,2 mm). El radio agua-equivalente  $R_w$  es un factor importante para Estimadores de Dosis Específicos del paciente (SSDE), se estimó teniendo en cuenta el espectro en cada maniquí. El ruido promedio de píxel se midió en regiones de interés (ROIs) de imágenes de maniqués de agua con radios de 2,5; 3; 6; 8 y 11,5 cm. Se encontró una asociación lineal entre  $C_{pmma,p}$  y  $C_{pmma,c}$ . Se describe una reducción de dosis a  $C_{pmma,c} = 2$  mGy por rotación del tubo mediante el análisis de datos (modo cabeza), con  $F_1 = 50$  mAs,  $F_3 = 19,2$  mm, resultando en un ruido promedio de píxel de 20 Unidades Hounsfield (UH).

**Palabras clave:** optimización; dosimetría; espectros de rayos X; tomografía computarizada; tratamiento de imágenes.

## Introduction

The operational process of clinical CT imaging is supported by a patient – technology – observers system with specific interactions of several factors (e.g. attributes of patient, x ray spectrum and its modulation, reconstruction algorithms and image quality perception) [1], affecting dosimetric and image quality quantities. Knowledge of quantitative association between CT dosimetric and image quality quantities with systemic factors, constitutes the basis to devise scanner-specific optimization strategies. Most of CT dosimetric quantities are derived from CT air kerma index ( $C_{pmma,c}$  at the center and  $C_{pmma,p}$  at the periphery) [2]. The aim was to analyze the association of the air kerma index with systemic factors and pixel noise, to get insight for specific optimization strategies.

## Materials and methods

Kerma indexes ( $C_{a,100}$  and  $C_{pmma,x}$ ) [2] were measured with a pencil ionization chamber (PTW-Freiburg, model TN30009-0577, 3,14 cm<sup>3</sup>), and an electrometer Unidos E (PTW-Freiburg) on both standard circular cylindrical PMMA phantoms with radius of 8 and 16 cm. A systemic approach was considered [1], regarding the following factors from a CT unit Siemens Sensation 64 Cardiac:

- 1 tube current x time product  $F_1$  (40 - 350 mAs), total collimation projected at isocenter  $F_3$  (2,7 - 19,2 mm), slice thickness  $F_7$  (0,15 - 1 cm), tube potential  $F_8$  (80 and 140 kV), and
- 2 the impinging spectrum  $\Phi_0$  was estimated with SPEKTR 3.0 [3] at the exit of the x ray tube, with added thickness of 0,2; 0,25 and 0,3 mm Cu, considering beam qualities as RQT 8 for measurements with 80 kV and 100 kV, RQT 9 for 120 kV and RQT 10 for 140 kV [2], respectively. The attenuated spectrum  $\Phi$  was computed for every phantom diameters and combinations of operational factors used for measurements. Additionally, the  $\Phi_0$  and  $\Phi$  were attenuated with specific inherent filtration, the latter computed using the MATLAB function *spektrTuner* [3], in order to satisfy the measured  $C_{a,100}$  and  $C_{pmma,c}$ . For the estimation of attenuated

spectrums, the phantom radius was considered as a layer thickness, traversed by all incident photons summed during one rotation of the x ray tube, but with fixed position of the x ray tube.

As  $C_{pmma,c}$  and  $C_{pmma,p}$  were measured in PMMA phantoms, and pixel noise measured in water phantoms, it is convenient to estimate the water equivalent radius  $R_w$ , which is here the thickness of a water layer that produces the same exposure attenuation that the PMMA layer under the same technical conditions (tube potential, tube current, collimation, and filtration).

It is very important that the uncertainty associated with the measurements be known and small. Through this work the measurement uncertainties express the 95 % confidence limits of the results, in case of used coverage factor  $k = 2$  will be addressed.

Average pixel noise  $\sigma$  was estimated from measurements with ROIs of 30 x 30 pixels in five positions (center, 12h, 3h, 6h and 9h) inside images of water phantoms with radius of 2,5; 3; 6; 8 and 11,5 cm. The same water phantoms were used in a previous work [4].

Data analysis was the departure to get insight for optimization alternatives. The association between  $C_{pmma,c}$  and  $C_{pmma,p}$  was verified graphically and with linear regression analysis. The association of  $C_{pmma,c}$  with  $F_1$ ,  $F_3$  and  $\sigma$  was verified with nonlinear regression analysis, with fixed values of tube potential and phantom radius.

## Results and discussion

The expanded uncertainties of  $C_{a,100}$  and  $C_{pmma,c}$  were 10,8 % and 12,4 % ( $k=2$ ) respectively (see details in table 1).

The total fluences were derived with spectrums obtained for all observations (see sample in figure 1 a), and each  $R_{w,i}$  was computed, corresponding to combinations of PMMA phantom radius and scanning factors  $F_1$ ,  $F_3$  and  $F_8$ . For PMMA layers of 8 cm and 16 cm the  $R_w$  were  $8,3 \pm 0,21$  cm and  $17,4 \pm 0,26$  cm respectively.

The quantity  $C_{vol}$  [2], wich takes into account the helical pitch or axial scan spacing, is linearly associated with  $C_{pmma,c}$ . Also a linear association was found here between measured  $C_{pmma,p}$  and  $C_{pmma,c}$  (see figure 1b).

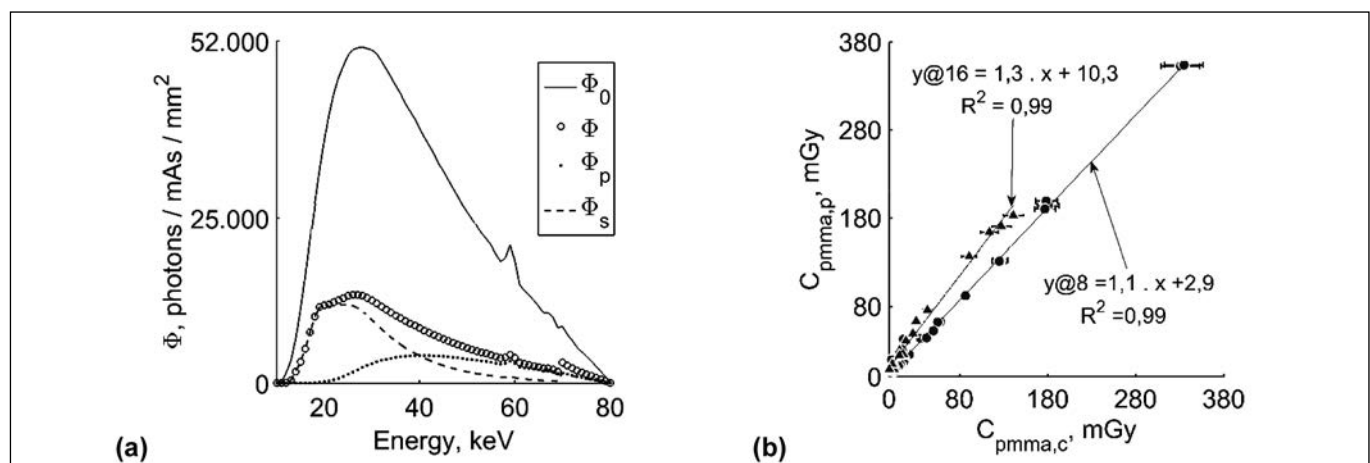


**Figure 1.** (a) Computed tungsten 80kVp spectrum: incident  $\Phi_0$  (which satisfies  $C_{a,100}$ ), spectrum  $\Phi$  that satisfies measured  $C_{pmma,c}$ , spectrum of primary radiation  $\Phi_p$  ( $\Phi$  attenuated with  $R_{pmma}$ ) and spectrum of scattered radiation  $\Phi_s$  ( $\Phi - \Phi_p$ ). (b) Linear association of  $C_{pmma,p}$  with  $C_{pmma,c}$ .

**Table 1.** Uncertainty budget for direct measurement of  $C_{pmma,p}$  and  $C_{pmma,c}$  using the ionization chamber – electrometer system (i.c.- e)

Source of uncertainty	Source for evaluation	Type	Uncertainty (k=1) [%]
Calibration factor of ionization chamber: $u_{calib}$	Calibration certificate	B	3,7
Differences of beam qualities between SSDL <sup>1</sup> and measurements: $u_{kQ}$	Calibration certificate	B	0,3
Direction of radiation incidence: $u_{dir}$	From [1]	B	1,0
Air pressure: $u_{pre}$	From [1]	B	0,5
Temperature and humidity: $u_{thu}$	From [1]	B	0,5
Electromagnetic compatibility: $u_{cel}$	From [1]	B	2,9
Field size/field homogeneity: $u_{hca}$	From [1]	B	1,0
Operating voltage of the system i.c.- e: $u_{vol}$	From [1]	B	1,2
Long term stability of user's instrument: $u_{est}$	From [1]	B	1,2
Precision of Reading in air: $u_{Mai}$	From [1]	A	1,0
Precision of tube loading indication: $u_{car}$	From [1]	B	1,0
Relative combined standard uncertainty (k = 1) for $C_{a,100}$			5,4
Relative expanded uncertainty (k = 2) for $C_{a,100}$			10,8
Precision of chamber/phantom positioning in the center of the gantry: $u_{pos}$	From [1]	B	0,3
Uncertainty of 1 mm in phantom diameter and 0.5 mm in depth of measurement bores: $u_{php}$	From [1]	B	0,4
Uncertainty in chamber response for in phantom measurements: $u_{plm}$	From [1]	B	3,0
Relative combined standard uncertainty (k = 1) for $C_{pmma,c}$			6,2
Relative expanded uncertainty (k = 2) for $C_{pmma,c}$			<b>12,4</b>

<sup>1</sup>SSDL – Secondary Standard Dosimetry Laboratory.

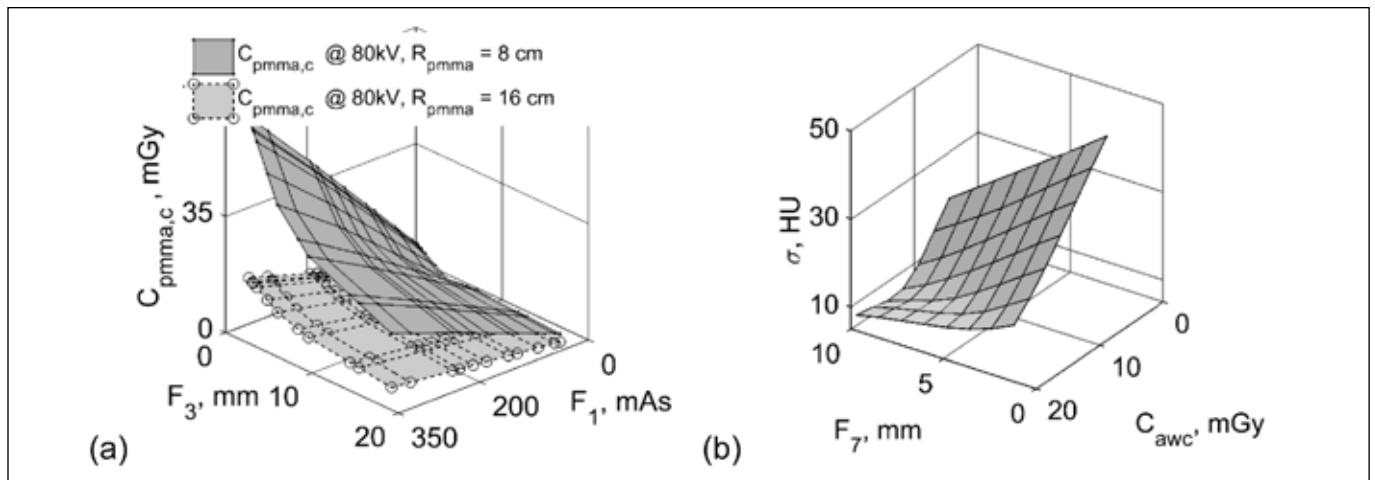


**Figure 2.** (a) Surfaces of  $C_{pmma,c}$  associated with  $F_1$ ,  $F_3$  and both diameters of standard PMMA phantoms and (b) the average pixel noise associated to  $C_{pmma,c}$  (represented by  $C_{awc} = C_{pmmac}$ , which is associated with  $R_w$ ) and the Slice Thickness  $F_7$ .

A good agreement between  $C_{pmma,p}$  and  $C_{pmma,c}$  was found for both phantom diameters of 8 cm and 16 cm, represented by the linear regression models  $y@8$  and  $y@16$  respectively in figure 1b.

The figure 2 a confirms that  $C_{pmma,c}$  has a direct linear association with  $F_1$  and is inversely proportional to  $F_3$ . Specifically for this example, the steeped surface for  $R_{pmma} = 8$  cm allows to identify, quantitatively, the operational regions with lower doses for pediatric examinations at 80 kV (e.g., less than 100 mAs and more than 10 mm of total collimation). In figure 2 b is represented the association of mean pixel noise  $\sigma$  with kerma at the center of a water phantom  $C_{awc}$  with  $R_w = 11,5$  cm. The  $C_{awc}$  was simulated using the spectrums of 80 kVp. The  $\sigma$

corresponds with a Reconstruction Diameter  $F_6 = 30$  cm and kernel H30s. A minimum  $C_{awc}$  is feasible with a resulting average pixel noise of 20 HU ( $F_1 = 50$  mAs and  $F_3 = 19,2$  mm).

## Conclusions

The spectrums matched with  $C_{a,100}$  and  $C_{pmma,x}$  allow to know quantitatively the contributions of primary and scattered radiation, and to estimate water equivalent radius adaptive to size specific quantities. This provides a basis for further modeling of dosimetric quantities and departure spectrums for in silico simulations when manufacturer data are not available. Knowledge of noise association

with  $C_{pmm,c}$  provides a straightforward tool for quantitative optimization, considering a systemic approach, including a patient - technology - observer system.

## Acknowledgement

This work was supported by the Centro de Biofísica Medica, as part of the project "Optimization of the image quality with respect to dose for pediatric Computed Tomography" (Code I 223 SC 904-002).

## References

- [1] MILLER-CLEMENTE RA, PÉREZ-DÍAZ M, GUEVARA MVM. AMAR: a systemic approach for patient radiation protection in CT. INIS 43(2010). Available in: <http://www.irpa12.org/fullpapers/FP3389.pdf>
- [2] IAEA. Dosimetry in diagnostic radiology: an international code of practice. TRS 457. Vienna: IAEA, 2007.
- [3] PUNNOOSE J, XU J, SISNIEGA A, ZBIJEWSKI W, et. al. Technical Note: spektr 3.0-A computational tool for x-ray spectrum modeling and analysis. Med Phys. 2016; 43: 4711-4717.
- [4] MILLER-CLEMENTE RA, PEREZ-DIAZ M, ZAMORA-MATAMOROS L, EDYVEAN S. Nonlinear model of image noise: an application on computed tomography including beam hardening and image processing algorithms. Applied Mathematics 2014; 5: 1320-1331.

**Recibido:** 13 de febrero de 2018

**Aceptado:** 29 de mayo de 2018